

'Entropically' stabilized region on the energy landscape of an ionic solid

This article has been downloaded from IOPscience. Please scroll down to see the full text article.

2003 J. Phys.: Condens. Matter 15 5479

(<http://iopscience.iop.org/0953-8984/15/32/309>)

View [the table of contents for this issue](#), or go to the [journal homepage](#) for more

Download details:

IP Address: 171.66.16.125

The article was downloaded on 19/05/2010 at 15:00

Please note that [terms and conditions apply](#).

‘Entropically’ stabilized region on the energy landscape of an ionic solid

J C Schön, M A C Wevers¹ and M Jansen

Max-Planck-Institut für Festkörperforschung, Heisenbergstraße 1, D-70569 Stuttgart, Germany

Received 1 April 2003

Published 1 August 2003

Online at stacks.iop.org/JPhysCM/15/5479

Abstract

High-dimensional energy landscapes of complex systems often exhibit a very complicated barrier structure. For the analysis of the dynamics on such landscapes, purely ‘energetic’ considerations are no longer sufficient, and ‘entropic’ and/or ‘dynamical’ contributions must be taken into account. We show how such ‘non-energetic’ barriers should be treated on a conceptually equal footing with classical ‘energetic’ barriers, and present a region belonging to a simple model of a crystalline compound, CaF₂, which is stabilized by ‘non-energetic’ barriers alone.

1. Introduction

Knowledge of the structure and properties of energy hypersurfaces is important for understanding the dynamic and static features of a large variety of complex physical and chemical systems [1–5]. Examples range from the relaxation dynamics in glasses [6–8] and spin glasses [9], over the folding transformation in proteins [10], and the study of the properties of clusters [11], polymers [12], and solids [13], to the efficiency of combinatorial optimization algorithms [14–16]. Due to the complexity of such landscapes, an analysis of their barrier structure by a simple scale-up of methods applicable to few-minima systems [17–19] soon reaches its limits, in particular when ‘non-energetic’ contributions to the barriers separating locally ergodic regions need to be taken into account. The hallmarks of such barriers in experiments and computer simulations are local equilibration within regions of the landscape corresponding to ‘energetically’ unstable structures, and very slow dynamics during transitions between locally ergodic regions, where the escape and transition times, respectively, do not follow an Arrhenius-like behaviour as a function of temperature.

The qualitative and quantitative aspects of such additional ‘barriers’ (sometimes denoted ‘entropic’ and/or ‘dynamical’) belong to the major open conceptual questions in the field of complex energy landscapes, from the original studies of two-state systems [20–22], and their generalizations to multiple basins [23, 24], to the large-scale simulations of glass models of varying complexity undertaken today [25–27]. For the simplest instance, a single saddle

¹ Present address: VDI-Technologiezentrum, Graf-Recke-Straße 84, D-40239 Düsseldorf, Germany.

point connecting two local minima, one can use transition state theory [20–22] to define ‘free energies’ of activation [23]. More systematic mathematical approaches [28–30] analyse the probability flow across normally hyperbolic invariant manifolds that separate the two minimum regions. Extending this approach by accounting for each saddle point separately, rather quickly becomes a nearly impossible task, in particular, if higher ranking saddles need to be included. Furthermore, the local properties of individual saddle points, e.g. their energies and curvatures, might not represent the appropriate quantitative measure of the corresponding transition region’s influence on the dynamics of the system on the timescales of interest.

In this context, one should note that usually one is only able to sample a small subset of the full landscape when studying complex energy landscapes on a global level. Thus, the ‘effective’ landscape one observes using various exploration methods might depend on the specific procedure one employs. For instance, the sets of local minima and saddle points one detects, e.g. by quenching from a constant temperature Monte Carlo (MC) or MD run, by performing slow annealing runs, by searching along exhaustive search cross sections of the landscape [31], by studying energy fluctuations [32], or by employing the threshold algorithm [33, 34], will usually be different. As a consequence, when modelling e.g. the long-time constant temperature dynamics from these data, one needs to take the origin of the information into account. In particular, the modelling step from the sampled minima and saddle points to the stochastic dynamics might not be straightforward, as mentioned above.

Keeping this in mind, we will focus on the flow of probability on the landscape, and the timescales associated with the corresponding stochastic dynamics, instead. We will present a specific example of a metastable structure on the energy landscape of a crystalline system, CaF_2 , where the analysis of the stochastic trajectories clearly shows that the structure is stabilized by ‘entropic’ barriers alone. As a consequence, this suggests the introduction of the concept of a ‘generalized’ barrier, which allows us to treat ‘energetic’ and ‘entropic’ barriers on the same footing.

2. ‘Entropically’ stabilized region for CaF_2

Of particular fascination are landscapes with locally ergodic regions, which are not stabilized via standard ‘energetic’ barriers B_E . As a specific instance of this type, we analyse a region belonging to the energy landscape of a simple model for CaF_2 , which may be the first clear-cut example of a non-amorphous structure stabilized by ‘non-energetic’ barriers alone. The global structure of this landscape has been investigated in earlier work [35, 36], and we refer to that work for details regarding the geometric structures of the minima (see figure 1) and the parameters in the potential energy (the interaction between the ions consisted of two-body terms: Coulomb-plus Lennard-Jones-interaction). Figure 1 shows the major global features of the landscape in a single-lump tree graph representation [34], as one finds when exploring the landscape with the threshold algorithm. All landscape explorations—simulated annealing runs, quench runs, threshold runs, and constant temperature MC simulations—were performed using stochastic algorithms based on the MC algorithm. The ‘moveclass’ consisted of (small) random displacements of individual atoms and random changes in the (periodically repeated) simulation cell.

During the search for local minima on the landscape of CaF_2 with simulated annealing [35], the optimization runs frequently yielded a certain structure, ‘VII-a’ (closely related to the stable local minimum VII-a in the MgF_2 system [35–37]), which appeared to be essentially unchanged after the relatively short ($< 10^4$ MC-steps) final quench phase of the optimization procedure².

² The fact that the ‘VII-a’-structure was observed during optimizations both with two and four formula units in the simulation cell is a further sign of the stability of this region on the landscape.

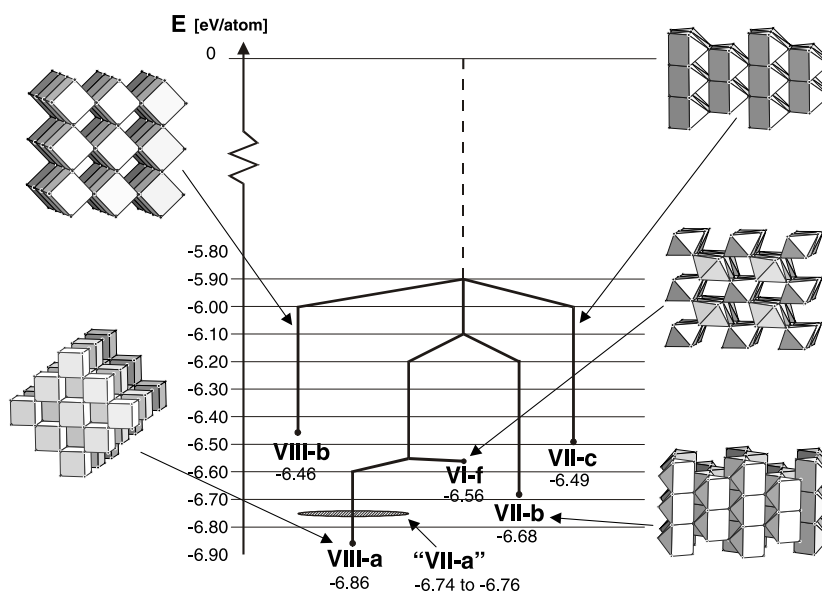


Figure 1. Tree graph diagram representation of the global structure of the energy landscape of the simplified CaF_2 -model. Minimum energy configurations are also depicted (for crystallographic details, see [35]). The shaded ellipse represents the energy range of the region ‘VII-a’ stabilized by ‘non-energetic’ barriers.

However, extensive investigations of the stability of the ‘VII-a’-structure with very long quench runs (5×10^4 MC-steps) showed that this structure candidate did not correspond to a local minimum of the potential energy [36]. Instead it was always transformed into the global minimum of the CaF_2 system, the fluorite structure (VIII-a).

At the same time, we employed the threshold algorithm [33] to investigate the stability of the other structure candidates in the CaF_2 -system. We observed that during essentially all of the quench runs that ended in the global minimum, the system resided for a considerable amount of time in a well-defined energy range between -6.74 and -6.76 eV/atom. The configurations in this region again exhibited the ‘VII-a’ structure.

In order to analyse this region in configuration space in more detail, in this work we have performed many threshold and MC simulations starting from points in the part of the landscape containing the regions VI-f, ‘VII-a’, and VIII-a. In particular, we have closely studied many instances of paths (both threshold and MC trajectories) taken by the system during the transition from VI-f to VIII-a in the CaF_2 -system. A few typical runs are shown in figure 2. Similar to the saddle region connecting VII-a to VI-a in the MgF_2 -system [36, 37], the energetic barrier is very low but the time to cross the saddle can be quite long. The trajectory soon reaches a region, from where all subsequent quenches will end up in VIII-a. For about 90% of the quench runs, the region ‘VII-a’ is encountered before the global minimum is reached (figure 2(a)). Subsequently, a rather long time τ_{esc} is spent there searching for an exit³, which implies the existence of substantial barriers separating this region from the minimum VIII-a.

³ During τ_{esc} , the coordination number for the two (crystallographically independent) cations changes from (6, 6) to (8, 7 + 1), and the atomic arrangement is transformed from a twisted sixfold coordination like in CaCl_2 via a VII-a-like structure to fluorite (see figure 2(d)). After this has been achieved, only small adjustments of atom–atom distances and some angles of the ‘pre-fluorite’ configuration are necessary to reach the fluorite structure.

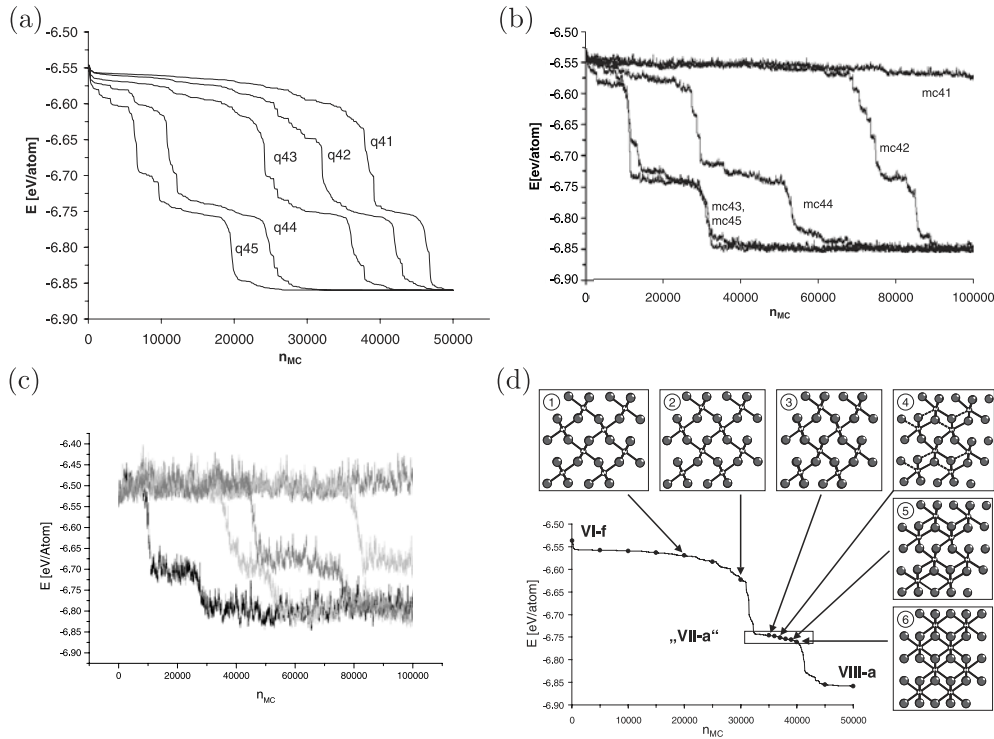


Figure 2. Energy E versus number of MC-steps n_{MC} for typical runs in CaF_2 , starting slightly above the saddle region connecting $VI-f$ to $VIII-a$. (a), (b), and (c) correspond to $T = 0$, 0.001, and 0.006 eV/atom, respectively. (d) For six points along a typical trajectory, the corresponding configurations are shown. Numbers 1 and 6 depict somewhat distorted CaCl_2 - and fluorite-structures, respectively. For the intermediate range (-6.74 to -6.76 eV/atom), we find a structure analogous to $VII-a$ in MgF_2 (number 4).

Since every quench run succeeded in leaving ‘ $VII-a$ ’ in the end, it is obvious that ‘non-energetic’ barriers of some kind are needed to stabilize this (intermediate) region. The results of the simulated annealing runs [35] indicate that most likely some rather high local density of states is present in this region, while the long time the quench runs take to cross this region suggests a rather complicated ‘microstructure’ in this region. Thus ‘entropic’ and ‘dynamical’ barriers B_S and B_D appear to contribute to the stability of the region.

The MC runs (of length 10^5 MC steps) performed at low temperatures for CaF_2 (see figures 2(b) and (c)) yielded strong corroborating evidence for the existence of large ‘non-energetic’ barriers. The system spends a long time (up to about 3×10^4 steps) in an intermediate energy range between about -6.71 and -6.75 eV/atom for $T = 0.001$ eV/atom, and about -6.73 to -6.62 eV/atom for $T = 0.006$ eV/atom. Note that these energies exceed those observed in the quench runs by an amount $O(n_f k_B T/2)$, where n_f is the number of degrees of freedom of the system. A clear sign that this slow transition dynamics is not due to ‘energetic’ barriers is the observation that the average escape times from region ‘ $VII-a$ ’ strongly increase with temperature: $\langle \tau_{esc} \rangle(T = 0) = 8.5 \times 10^3$, $\langle \tau_{esc} \rangle(T = 0.001) = 15.8 \times 10^3$, and $\langle \tau_{esc} \rangle(T = 0.006) = 18.5 \times 10^3$. This temperature dependence is exactly opposite to what one would expect for ‘energetic’ barriers, and it is consistent with the fact that the system does not easily escape from the region ‘ $VII-a$ ’ during the simulated annealing runs.

3. Generalized barriers

The system presented above clearly shows that ‘non-energetic’ barriers can play a decisive role in the dynamical behaviour of a system. In particular, the results suggest that one needs a unified approach that allows us to treat ‘energetic’, ‘entropic’ and ‘dynamical’ barriers on an equal footing. In order to achieve this goal, our general approach focuses on the flow of probability on the landscape, and the timescales associated with the corresponding stochastic dynamics, instead of the classical energy barriers and saddles between local minima. We assume in the following that the system is in contact with a heat bath and is essentially fully damped, resulting in a hopping dynamics on the potential energy landscape that can be described with sufficient accuracy by a constant temperature MC algorithm⁴.

When analysing the dynamics on landscapes, one very useful step is the coarsening of the landscape by dividing it into sub-regions, whose internal dynamics and whose interactions among each other can be described by a few parameters. These sub-regions can be classified into two types: locally ergodic regions [4, 39], which equilibrate on timescales short compared to the escape time from the region, $\tau_{\text{eq}} < \tau_{\text{obs}} \ll \tau_{\text{esc}}$, and transition regions, where the equilibration time exceeds the average escape time. Of course, these sub-regions can be quite extended, e.g. containing many local minima, if the relevant observational timescale τ_{obs} is large. Knowledge of the average escape times from these regions and the associated probabilities to exit from e.g. region \mathcal{A} to \mathcal{B} allow us to model the time evolution on large timescales as a probabilistic dynamics described by a Markov process [38].

Thus, instead of trying to construct ‘energetic’, ‘entropic’, and ‘dynamical’ barriers from the geometry of the landscape, we place all these barriers on an equal footing by treating the escape times (for locally ergodic regions) and transition times (for transition regions) as the primary quantities, and use these to define a generalized barrier via⁵,

$$B(T; \mathcal{R}) \propto \ln(\tau(T; \mathcal{R})). \quad (1)$$

For locally ergodic regions, the escape time is averaged over all points within the region weighted by the appropriate statistical distribution, while for transition regions, we need to determine separate transition times for each entrance set of points because of the lack of local ergodicity. Of course, for simple regions, we can try to compute or estimate such barriers analytically, and identify typical contributions, $B_1(T)$, $B_2(T)$, etc, labelling them as e.g. ‘energetic’, ‘entropic’, or ‘dynamical’. Note that, in general, these ‘barriers’ are not additive, $B(T; \mathcal{R}) \neq B_1 + B_2 + \dots$, since the escape time can usually not be written as a product of independent timescales, $\tau_{\text{esc}} \neq \tau_1 \tau_2 \dots$.

To illustrate this approach, consider a locally ergodic minimum region \mathcal{A} with $N_{\mathcal{A}}$ states (E_{b} = energy of minimum), sharing a surface \mathcal{S} consisting of $N_{\mathcal{S}}$ states⁶ at an energy E_{t} with a transition region \mathcal{G} , where the total number of states at energy E_{t} and E_{b} belonging to \mathcal{A} is N_{t} and N_{b} , respectively. The surface \mathcal{S} is defined as the set of all those points for which the probabilities, in a stochastic dynamics, to return to \mathcal{A} or to enter \mathcal{G} are equal (1/2). The escape time from \mathcal{A} via \mathcal{S} would thus correspond to the average time needed to reach \mathcal{S} from points within \mathcal{A} . Since we are dealing with a locally ergodic region, $\tau_{\text{esc}} \gg \tau_{\text{eq}}$. Thus we can assume

⁴ However, many of the considerations should also apply to more general types of dynamics [38].

⁵ The unit of time is incorporated in the proportionality factor of equation (1). For modelling purposes, time might be measured in MC-steps, or the inverse of the highest vibrational frequency, etc.

⁶ In general, \mathcal{S} will consist of several disconnected pieces. Furthermore, the points in \mathcal{S} will, in general, belong to a whole range of energies $[E_{\text{t}}, E_{\text{t}} + \Delta]$.

that

- (a) the states in \mathcal{A} are occupied according to the Boltzmann distribution and the thermodynamic weight of region \mathcal{A} is given by the sum over states $Z(\mathcal{A})$ restricted to \mathcal{A} . Furthermore,
- (b) the timescale τ_D for movement within \mathcal{A} (reflecting the internal structure of \mathcal{A}) should be comparable to τ_{eq} , $\tau_D \approx \tau_{\text{eq}}$, and thus can be neglected when estimating τ_{esc} .

It follows that

$$\tau_{\text{esc}} \propto \frac{Z(\mathcal{A})}{N_S \exp(-E_t/T)} = \frac{Z(\mathcal{A})}{N_t \exp(-E_t/T)} \times \frac{N_t}{N_S} = \tau_1 \tau_2, \quad (2)$$

and the corresponding generalized barrier can be written as a sum of two terms,

$$B = \ln\left(\frac{Z(\mathcal{A})}{N_t \exp(-E_t/T)}\right) + \ln\left(\frac{N_t}{N_S}\right) = B_1 + B_2. \quad (3)$$

The first term denotes the timescale on which the system will reach the energy range E_t of the exit surface \mathcal{S} with probability $\text{O}(1)$. For non-exponential growth in the local density of states of \mathcal{A} , $g_{\mathcal{A}}(E)$, we can approximate this as⁷ $B_1 = B_E \approx (E_t - E_b)/T - \ln(N_t/N_b)$. For $(E_t - E_b)/T \gg \ln(N_t/N_b)$, B_E represents a purely ‘energetic’ barrier with an activation energy $E_t - E_b$. However, in the case of $g_{\mathcal{A}}(E) \propto \exp(\alpha(E - E_b))$, this interpretation only applies for temperatures below the trapping temperature $T < T_{\text{trap}} = 1/\alpha$ [14, 15]; else, for $T > 1/\alpha$, the system is found at $E = E_t$ with overwhelming probability, i.e. the ‘energetic’ contribution to B can be neglected.

The second term, $B_2 = \ln(N_t/N_S) \approx \ln(N_{\mathcal{A}}/N_S)$, is a measure of the (inverse) probability of visiting one of the N_S points of the exit surface \mathcal{S} once the energy E_t has been reached. Since B_2 only depends on the relative sizes of the exit surface and the total region, it might reasonably be called an ‘entropic’ barrier B_S . We note that we could interpret $N_{\mathcal{A}}/N_S$ as the average time needed by a random walker on an ideal structureless (e.g. a fully connected) graph to reach a specified set of N_S points with probability $\text{O}(1)$, $\tau_2 = \tau_{\text{diff}}^{\text{ideal}}$.

In principle, one would need to take the real, possibly rather involved connectivity of \mathcal{A} into account⁸, $\tau_2 = \tau_{\text{diff}}^{\text{real}} \geq \tau_{\text{diff}}^{\text{ideal}}$. Because of the local ergodicity of \mathcal{A} , $\tau_{\text{diff}}^{\text{real}} \approx \tau_{\text{diff}}^{\text{ideal}}$ in this particular instance. But this is no longer the case for transition regions, and one needs to solve the corresponding diffusion problem in order to determine τ_2 . In this work, we refrain from presenting specific analytically solvable examples of transition regions. Detailed analyses of a number of such examples that might be useful as building-blocks when modelling realistic transition regions are given in [38].

4. Discussion

While the metastable phases in the CaF_2 system have not yet been explored experimentally, there exist closely related AB_2 systems that exhibit (meta)stable compounds analogous to those we find on the energy landscape of CaF_2 . One such interesting application of our analysis is the possible intermediates in the high pressure phase transition of RuO_2 from rutile over a CaCl_2 -intermediate to the fluorite structure [40]. The second step along that path corresponds exactly to the *VI-f* \rightarrow *VIII-a* transition we have discussed. Our results suggest that an (‘entropically’ stabilized) structure like *VII-a* might occur as a second intermediate between CaCl_2 and fluorite.

⁷ For continuous systems at finite temperatures, N_b and N_t would correspond to the number of states within a band of $\text{O}(k_B T)$ around E_b and E_t , respectively. Similarly, \mathcal{S} will possess a finite volume in state space.

⁸ In some cases, it can be useful to define $B_D = \ln(\tau_{\text{diff}}^{\text{real}}/\tau_{\text{diff}}^{\text{ideal}})$ as a ‘dynamical’ barrier, representing the effect of the internal structure of \mathcal{A} .

Our conclusion actually supports the proposal by Haines and Léger [40], who have suggested a hypothetical intermediate very similar to our *VII-a*-structure along one proposed transition route. In addition, they observed very slow kinetics of the phase transformation, which is a first hint that the transition region might be stabilized by 'non-energetic' barriers.

The region '*VII-a*' in the CaF₂ system appears to be perhaps the first clear-cut example of a structurally well-defined region on an energy landscape of a physical system that is stabilized by purely 'non-energetic' barriers. In the past, either mixtures of 'entropic'/'dynamical' and 'energetic' barriers were present, e.g. for amorphous systems [7, 23, 25], where the 'non-energetic' barriers are expected to influence the glass transition [7, 8, 15, 27] and are a possible cause for aging phenomena in spin glasses [41], or one has dealt with structurally ill-defined 'liquid-like' states, e.g. dense hard-sphere systems [26].

Such 'non-energetic' barriers can also be found in systems with deterministic dynamics⁹ as recent investigations [42] of the phase space and timescales of seemingly simple systems consisting of a Cassini and a Sinai billiard show. Finally, generalized barriers of a landscape also play an important role in the success (or failure) of optimization algorithms [15, 16, 36], and when optimizing their design one needs to ensure that lowering 'energy' barriers does not raise equally troublesome 'entropic' or 'dynamical' barriers in their place.

Acknowledgments

We would like to acknowledge fruitful discussions at workshops on energy landscapes at the Telluride Summer Research Center in 1997, 1999, and 2001. This work was partly funded by the DFG via SFB408.

References

- [1] Frauenfelder H, Bishop A R, Garcia A, Perelson A, Schuster P, Sherrington D and Swart P J (ed) 1996 Landscape paradigms in physics and biology *Physica D* **107** (2–4)
- [2] Palmer R 1982 *Adv. Phys.* **31** 669
- [3] Wales D J, Doye J P K, Miller M A, Mortenson P N and Walsh T R 2000 *Advances in Chemical Physics* vol 115, ed I Prigogine and S A Rice (New York: Wiley) pp 1–111
- [4] Schön J C and Jansen M 2001 *Z. Kristallogr.* **216** 307
- [5] Schön J C and Jansen M 2001 *Z. Kristallogr.* **216** 361
- [6] Jäckle J 1986 *Rep. Prog. Phys.* **49** 171
- [7] Dasgupta C and Valls O T 1998 *Phys. Rev. E* **58** 801
- [8] Schön J C and Sibani P 1998 *J. Phys. A: Math. Gen.* **31** 8167
- [9] Sibani P 1998 *Physica A* **258** 249
- [10] Dobson C M, Sali A and Karplus M 1998 *Angew. Chem. Int. Edn. Engl.* **37** 868
- [11] Berry R S 1993 *Chem. Rev.* **93** 2379
- [12] Becker O M and Karplus M 1997 *J. Chem. Phys.* **106** 1495
- [13] Schön J C and Jansen M 1996 *Angew. Chem. Int. Edn. Engl.* **35** 1286
- [14] Sibani P, Schön J C, Salamon P and Andersson J-O 1993 *Europhys. Lett.* **22** 479
- [15] Schön J C 1997 *J. Phys. A: Math. Gen.* **30** 2367
- [16] Salamon P, Sibani P and Frost R 2002 *Facts, Conjectures, and Improvements for Simulated Annealing (SIAM Monographs)* (Philadelphia, PA: SIAM)
- [17] Davis H L, Wales D J and Berry R S 1990 *J. Chem. Phys.* **92** 4308
- [18] Cerjan C J and Miller W H 1981 *J. Chem. Phys.* **75** 2800
- [19] Quapp W 1996 *Chem. Phys. Lett.* **253** 286
- [20] Kramers H A 1940 *Physica* **VII** 284

⁹ Of course, any classical dynamical system that follows constant energy trajectories only encounters 'non-energetic' barriers. But the escape time from e.g. a local minimum is controlled by the anharmonic terms of the potential which destroy the invariant tori of the harmonic motion around the minimum [29]. Thus crossing a saddle region still involves an effective 'potential energy barrier'.

- [21] Rice S A 1958 *Phys. Rev.* **112** 804
- [22] Glyde H R 1967 *Rev. Mod. Phys.* **39** 373
- [23] Stillinger F H 1990 *Phys. Rev. B* **41** 2409
- [24] Mohanty U, Oppenheim I and Taubes C H 1994 *Science* **266** 425
- [25] Daldoss G, Pilla O, Viliiani G and Brangian C 1999 *Phys. Rev. B* **60** 3200
- [26] Dasgupta C and Valls O T 1999 *Phys. Rev. E* **59** 3123
- [27] Ritort F 1995 *Phys. Rev. Lett.* **75** 1190
- [28] Pollak E and Pechukas P 1978 *J. Chem. Phys.* **69** 1218
- [29] Komatsuzaki T and Berry R S 2000 *J. Mol. Struct. (Theochem)* **506** 55
- [30] Wiggins S, Wiesenfeld L, Jaffé C and Uzer T 2001 *Phys. Rev. Lett.* **86** 5478
- [31] Schön J C and Sibani P 2000 *Europhys. Lett.* **49** 196
- [32] Dall J and Sibani P 2003 *J. Phys.: Condens. Matter* submitted
(Dall J and Sibani P 2003 *Preprint*)
- [33] Schön J C 1996 *Ber. Bunsenges.* **100** 1388
- [34] Schön J C, Putz H and Jansen M 1996 *J. Phys.: Condens. Matter* **8** 143
- [35] Wevers M A C, Schön J C and Jansen M 1998 *J. Solid State Chem.* **136** 223
- [36] Wevers M A C, Schön J C and Jansen M 1999 *J. Phys.: Condens. Matter* **11** 6487
- [37] Wevers M A C, Schön J C and Jansen M 2001 *J. Phys. A: Math. Gen.* **34** 4041
- [38] Schön J C 2003 in preparation
- [39] Schön J C 1998 *Proc. RIGI-workshop 1998* ed J Schreuer, ETH Zürich, Zürich
- [40] Haines J and Léger J M 1993 *Phys. Rev. B* **48** 13344
- [41] Hoffmann K H, Schubert S and Sibani P 1997 *Europhys. Lett.* **38** 613
- [42] Zaslavsky G M and Edelman M 1997 *Phys. Rev. E* **56** 5310